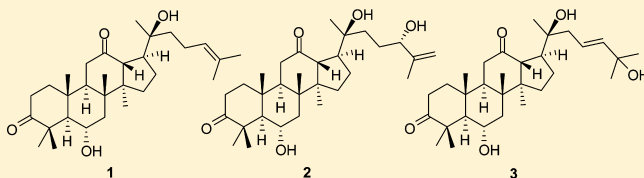


Dammarane Triterpenes as Potential SIRT1 Activators from the Leaves of *Panax ginseng*Jun-Li Yang,[†] Thi-Kim-Quy Ha,[†] Basanta Dhodary,[†] Kuk-Hwa Kim,[†] Junsoo Park,[‡] Chul-Ho Lee,[§] Young-Choong Kim,[†] and Won-Keun Oh^{*,†}[†]Korea Bioactive Natural Material Bank, Research Institute of Pharmaceutical Sciences, College of Pharmacy, Seoul National University, Seoul 151-742, Republic of Korea[‡]Division of Biological Science and Technology, Yonsei University, Wonju 220-100, Republic of Korea[§]Laboratory Animal Center, Korea Research Institute of Bioscience and Biotechnology, Yuseong-gu, Daejeon 305-806, Republic of Korea

S Supporting Information

ABSTRACT: During a search for SIRT1 activators originating in nature, three new dammarane triterpenes, 6 α ,20(S)-dihydroxydammar-3,12-dione-24-ene (**1**), 6 α ,20(S),24(S)-trihydroxydammar-3,12-dione-25-ene (**2**), and 6 α ,20(S),25-trihydroxydammar-3,12-dione-23-ene (**3**), as well as two known triterpenes, dammar-20(22),24-diene-3 β ,6 α ,12 β -triol (**4**) and 20(S)-ginsenoside Rg₃ (**5**), were isolated from *Panax ginseng* leaves. Compounds **1** and **3–5** showed potential as SIRT1 activators, as analyzed by in vitro enzyme-based SIRT1-NAD⁺/NADH and SIRT1-p53 luciferase cell-based assays. They were also found to increase the level of NAD⁺/NADH ratio in HEK293 cells. This study presents a new class of chemical entities that may be able to be developed as SIRT1 activators for antiaging and treatment of age-associated diseases.



SIRT1, a homologue of silent information regulator two (SIR2), is a NAD⁺ (nicotinamide adenine dinucleotide)-dependent class III histone deacetylase, which regulates cell survival and lifespan.^{1–3} SIRT1 plays a pivotal role in a variety of cellular processes including cellular aging, neuronal protection, and antiapoptosis by deacetylating nonhistone proteins, such as the forkhead transcription factor (FOXO), the RelA/p65 subunit of nuclear factor-kappa B (NF- κ B), and tumor suppressor p53.^{4,5} Once activated, SIRT1 can promote the potentiation of stress resistance and extend longevity through age-related metabolic regulation, including regulation of factors involved in cell survival, cardioprotection, neuroprotection, insulin secretion, glycolysis, and fat storage.^{6,7} Therefore, finding effective SIRT1 activators may be significant for combating the aging process, and for treating age-related diseases. To date, most of the known SIRT1 activators are synthetic entities, including 1,4-dihydropyridine,⁸ oxazolo[4,5-*b*]pyridine,⁹ imidazo[1,2-*b*]thiazole,¹⁰ thiazolopyridine,⁷ and benzimidazole derivatives.⁷ Only a limited number of naturally occurring small molecule SIRT1 activators have been reported, the majority of which are flavonoids and phenolic compounds.^{11,12} Among them, resveratrol was the first reported, and is the most common naturally occurring SIRT1 activator.^{12–14}

In a search for new SIRT1 activators from natural sources, four terpenylated coumarins from *Ailanthus altissima* were reported to enhance SIRT1 deacetylase activity.¹⁵ As part of our ongoing efforts, it was found that an ethanol extract of *Panax ginseng* leaves showed potential stimulatory effects on

SIRT1 deacetylase activity. *Panax ginseng* L. root (Araliaceae) is known as an important multifunctional therapeutic herb and health food commonly used in Korea, mainland China, and Japan and has been shown to have various pharmacological activities on aging, cancer, inflammation, and diabetes, as well as immunomodulatory action and effects on the cardiovascular system and the central nervous system.^{16–19} Herein are described the isolation, structure elucidation, and the potency as SIRT1 activators of the compounds (**1–5**) obtained from *P. ginseng* leaves.

RESULTS AND DISCUSSION

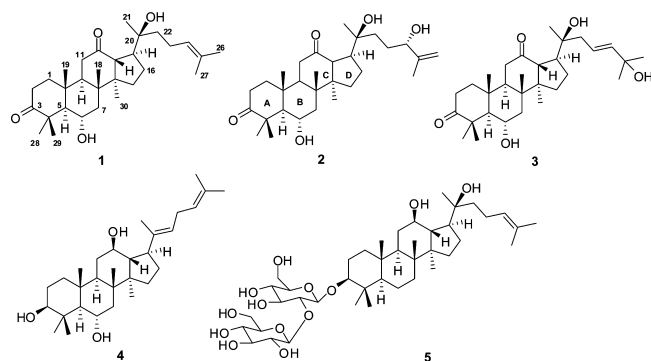
Bioassay-guided fractionation of the bioactive EtOH extract of *P. ginseng* leaves afforded three new triterpenes, 6 α ,20(S)-dihydroxydammar-3,12-dione-24-ene (**1**), 6 α ,20(S),24(S)-trihydroxydammar-3,12-dione-25-ene (**2**), and 6 α ,20(S),25-trihydroxydammar-3,12-dione-23-ene (**3**), along with two known triterpenes, dammar-20(22),24-diene-3 β ,6 α ,12 β -triol (**4**),²⁰ and 20(S)-ginsenoside Rg₃ (**5**).²¹ See Scheme 1 for structures.

Compound **1** was obtained as a white amorphous powder. Its molecular formula was determined as C₃₀H₄₈O₄ based on a quasimolecular ion peak at *m/z* 495.3457 [M + Na]⁺ (calcd for C₃₀H₄₈O₄Na, 495.3450) in the positive HRFABMS, suggesting seven degrees of unsaturation. The IR absorptions indicated the presence of OH (3397 cm⁻¹), C=O (1722, 1705 cm⁻¹), and

Received: March 11, 2014

Published: June 27, 2014

Scheme 1



C=C (1654 cm^{-1}) functionalities. The ^1H NMR data (Table 1) showed six tertiary methyl signals at δ_{H} 1.40, 1.39, 1.30, 1.17,

0.90, and 0.89, two methyls connected to an olefinic system at δ_{H} 1.73 and 1.67, an oxymethine proton at δ_{H} 4.15 (td, $J = 10.5$, 3.5 Hz), and an olefinic proton at δ_{H} 5.15 (t, $J = 6.5\text{ Hz}$). The ^{13}C NMR spectroscopic data (Table 1) displayed 30 carbon signals, including two ketone carbonyl carbons at δ_{C} 218.4 and 212.5, two olefinic carbons at δ_{C} 131.7 and 124.6, an oxymethine carbon at δ_{C} 67.6, and an sp^3 oxygenated quaternary carbon at δ_{C} 73.3. Detailed analysis of the above NMR information suggested that compound 1 possesses a similar A/B ring structure to panaxadiene.²² However, the C/D ring and the side-chain moieties of 1 resembled those of the 3-*O*-acetyl-12-keto derivative of betulafoletriol.²³ This analysis indicated that the carbonyl groups are connected to C-3 and C-12, respectively, with two hydroxy groups connected, in turn, to C-6 and C-20, and an olefinic system located between C-24 and C-25. This proposed arrangement was confirmed by HMBC correlations (Figure 1) from H-2 (δ_{H} 2.78), H₃-28 (δ_{H} 1.39),

Table 1. NMR Spectroscopic Data (500 MHz) for Compounds 1–3

position	1 ^a		2 ^b		3 ^b	
	δ_{H} (J in Hz)	δ_{C}	δ_{H} (J in Hz)	δ_{C}	δ_{H} (J in Hz)	δ_{C}
1	1.75, m 1.01, m	39.3, CH ₂	2.12, m 1.59, m	38.8, CH ₂	2.14, m 1.49, m	38.5, CH ₂
2	2.78, m 2.48, m	32.6, CH ₂	2.79, m 2.31, m	32.5, CH ₂	2.80, m 2.25, m	33.5, CH ₂
3		218.4, C		218.8, C		218.6, C
4		47.2, C		48.1, C		48.1, C
5	1.78, d (10.5)	58.6, CH	1.94, d (10.1)	59.1, CH	1.93, d (11.0)	59.1, CH
6	4.15, td (10.5, 3.5)	67.6, CH	4.28, m	67.2, CH	4.27, m	67.2, CH
7	2.34, m 1.92, m	43.9, CH ₂	2.37, m 1.87, m	45.1, CH ₂	2.33, m 1.87, m	45.0, CH ₂
8		40.7, C		41.5, C		41.6, C
9	1.93, m	51.8, CH	1.96, m	53.4, CH	1.99, m	53.4, CH
10		38.2, C		40.1, C		40.6, C
11	2.29, m 2.20, m	38.9, CH ₂	2.36, m 2.29, m	38.6, CH ₂	2.37, m 2.31, m	37.9, CH ₂
12		212.5, C		211.9, C		211.9, C
13	2.95, d (10.0)	55.6, CH	3.41, d (10.0)	56.5, CH	3.42, d (10.0)	56.4, CH
14		54.7, C		56.3, C		56.3, C
15	1.56, m 1.05, m	31.0, CH ₂	1.53, m 1.23, m	31.4, CH ₂	1.58, m 1.23, m	32.4, CH ₂
16	1.77, m 1.37, m	24.5, CH ₂	2.12, m 1.87, m	24.9, CH ₂	2.16, m 1.90, m	24.8, CH ₂
17	2.47, m	45.5, CH	2.80, m	44.4, CH	2.79, m	44.3, CH
18	1.30, s	16.7, CH ₃	1.24, s	16.9, CH ₃	1.26, s	16.5, CH ₃
19	0.89, s	17.1, CH ₃	0.82, s	17.3, CH ₃	0.83, s	17.1, CH ₃
20		73.3, C		73.7, C		74.0, C
21	1.17, s	26.3, CH ₃	1.46, s	27.3, CH ₃	1.46, s	27.6, CH ₃
22	2.08, m 1.32, m	38.0, CH ₂	1.95, m 1.49, m	39.7, CH ₂	2.61, m 2.54, m	46.0, CH ₂
23	2.16, m 2.08, m	22.5, CH ₂	2.02, m 1.17, m	33.5, CH ₂	6.25, m	123.2, CH
24	5.15, t (6.5)	124.6, CH	4.41, br t (5.0)	76.2, CH	6.02, d (15.4)	143.3, CH
25		131.7, C		150.7, C		70.2, C
26	1.73, s	25.7, CH ₃	5.28, br s 4.97, br s	110.5, CH ₂	1.53, s	31.3 ^c , CH ₃
27	1.67, s	17.1, CH ₃	1.90, br s	18.8, CH ₃	1.53, s	31.2 ^c , CH ₃
28	1.39, s	31.8, CH ₃	1.67, s	32.4, CH ₃	1.67, s	32.5, CH ₃
29	1.40, s	19.5, CH ₃	1.71, s	20.2, CH ₃	1.70, s	20.3, CH ₃
30	0.90, s	17.0, CH ₃	0.90, s	17.5, CH ₃	0.89, s	17.5, CH ₃

^aData were measured in CDCl_3 . ^bData were measured in $\text{C}_3\text{D}_5\text{N}$. ^cValues may be exchanged.

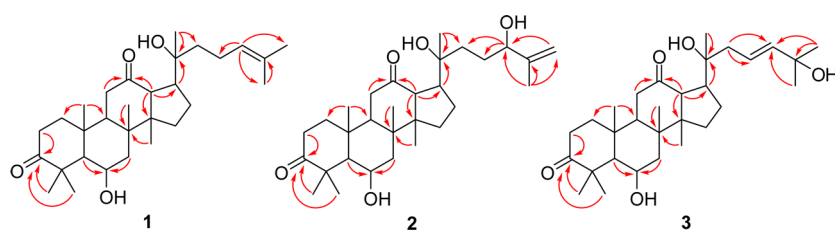


Figure 1. Key HMBC correlations (from H to C) for new compounds 1–3.

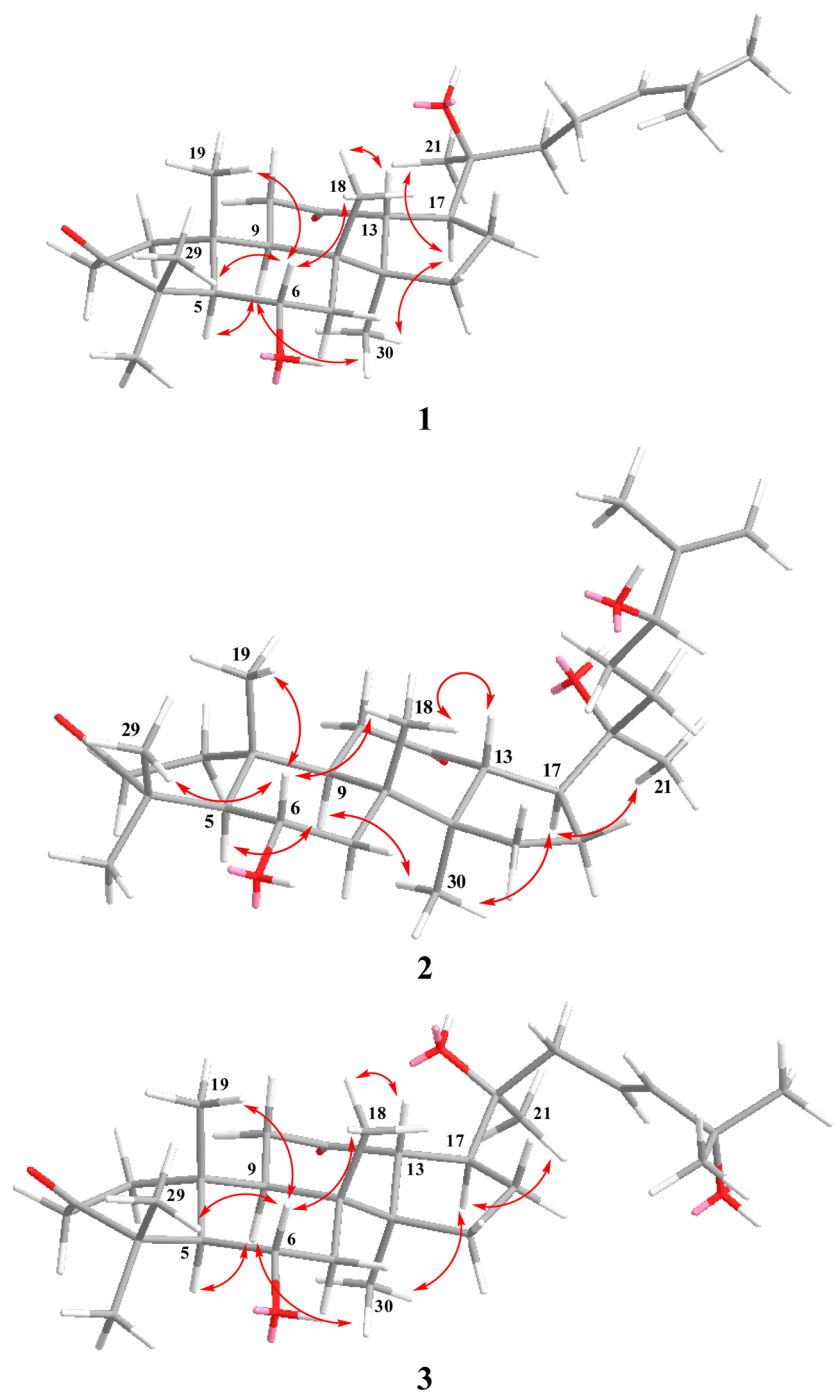


Figure 2. Key NOESY correlations for new compounds 1–3.

and H₃-29 (δ_{H} 1.40) to C-3 (δ_{C} 218.4), from H-5 (δ_{H} 1.78) and H-7 (δ_{H} 1.92) to C-6 (δ_{C} 67.6), from H-11 (δ_{H} 2.29) and H-13 (δ_{H} 2.95) to C-12 (δ_{C} 212.5), from H-17 (δ_{H} 2.47) and

H₃-21 (δ_{H} 1.17) to C-20 (δ_{C} 73.3), and from H-24 (δ_{H} 5.15) to C-26 (δ_{C} 25.7) and C-27 (δ_{C} 17.1). The coupling constant between H-5 and H-6 ($J = 10.5$ Hz) implied that H-6 should be

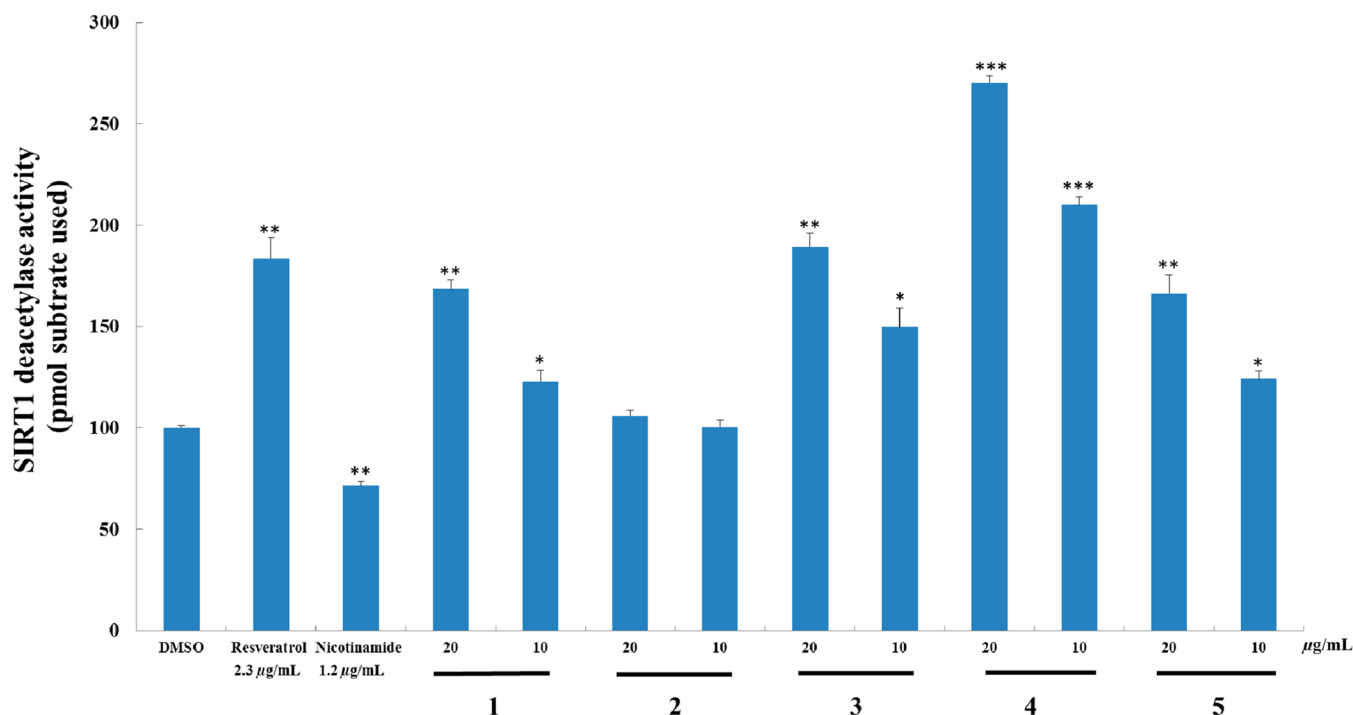


Figure 3. Effects of compounds 1–5 on SIRT1 enzymatic activities with a p53 peptide substrate in an in vitro SIRT1-NAD/NADH enzyme-based assay.

axial as in the case of H-5, which was also supported by NOESY correlations from H-6 to H₃-18, H₃-19, and H₃-29 (Figure 2), indicating OH-6 to be equatorial and α -oriented. In addition, the coupling constant between H-13 and H-17 ($J = 10.0$ Hz) and the NOESY correlations from H-13 to H₃-18 and from H-17 to H₃-21 and H₃-30 (Figure 2) supported the assignments of the α -oriented H-17 and of the C-20(*S*) configuration.²⁴ Thus, compound 1 was determined as 6 α ,20(*S*)-dihydroxydammar-3,12-dione-24-ene.

Compound 2, a white, amorphous powder, gave a quasimolecular ion at m/z 511.3409 [$M + Na$]⁺ (calcd for C₃₀H₄₈O₅Na, 511.3399) in the positive HRFABMS, consistent with a molecular formula of C₃₀H₄₈O₅, suggesting seven degrees of unsaturation. Its IR spectrum showed absorptions for OH (3362 cm⁻¹), C=O (1721, 1700 cm⁻¹), and C=C (1637 cm⁻¹) functionalities. Detailed analysis of the ¹H and ¹³C NMR data (Table 1) suggested compound 2 as having a similar structure to 1 except for their side chains, in which two ketone groups were located at C-3 and C-12, respectively, and one hydroxy group was identified at C-6. These results were supported by HMBC correlations, as follows (Figure 1): from H₂-2 (δ_H 2.79 and 2.31), H₃-28 (δ_H 1.67), and H₃-29 (δ_H 1.71) to C-3 (δ_C 218.8); from H-11 (δ_H 2.29), H-13 (δ_H 3.41), and H-17 (δ_H 2.80) to C-12 (δ_C 211.9); and from H-5 (δ_H 1.94) and H-7 (δ_H 1.87) to C-6 (δ_C 67.2). HSQC correlations from one pair of olefinic protons at δ_H 5.28 (br s) and 4.97 (br s) to a carbon at δ_C 110.5 and the deshielding of a methyl at δ_H 1.90 (br s) suggested the presence of a $\Delta^{25,26}$ olefinic system, and the signal at δ_H 1.90 was assigned as H₃-27, respectively. This observation was confirmed by HMBC correlations (Figure 1) from H₃-27 (δ_H 1.90) to C-25 (δ_C 150.7) and C-26 (δ_C 110.5). In addition, HMBC correlations from H₂-26 (δ_H 5.28 and 4.97) and H₃-27 (δ_H 1.90) to a signal at δ_C 76.2 demonstrated this carbon (δ_C 76.2) to be located at C-24 and suggested the presence of an OH-24 group in the structure. The other

hydroxy group was assigned as OH-20 on the basis of HMBC correlations from H-13 (δ_H 3.41), H-17 (δ_H 2.80), and H₃-21 (δ_H 1.46) to C-20 (δ_C 73.7). The relative configuration of compound 2 was determined by analyzing coupling constants and NOESY correlations, as well as by comparing the NMR data with literature values. The large coupling constant between H-5 and H-6 ($J = 10.1$ Hz) implied H-6 as being axial, indicating an equatorial α -orientation for OH-6. Similarly, H-17 was determined as being α -oriented based on the coupling pattern between H-13 and H-17 ($J = 10.0$ Hz). The same configuration of the C/D rings and the similar chemical shifts of C-17, C-20, C-21, and C-22 between compound 2 and the 3-*O*-acetyl-12-keto derivative of betulafoletriol²³ were used to support the assignment of a C-20(*S*) configuration.²⁴ The above inferences were supported further by the following NOESY correlations: from H-6 to H₃-18, H₃-19, and H₃-29; from H-13 to H₃-18; and from H-17 to H₃-21 and H₃-30 (Figure 2). The configuration at C-24 was determined by NMR data analysis.^{25,26} A chemical shift of C-24 in compound 2 (δ_C 76.2 in C₅D₅N) and 20(*S*),24(*S*)-dihydroxydammar-25-en-3-one²⁷ (δ_C 76.3 in C₅D₅N; 76.4 in CDCl₃), which was different from that of fouquierone (δ_C 89.7 in CDCl₃),²⁸ were used to establish the 24(*S*) configuration in 2. Thus, compound 2 was elucidated as 6 α ,20(*S*),24(*S*)-trihydroxydammar-3,12-dione-25-ene.

Compound 3, isolated as a white, amorphous powder, was found to possess a molecular formula of C₃₀H₄₈O₅ based on the quasimolecular ion at m/z 511.3346 [$M + Na$]⁺ (calcd for C₃₀H₄₈O₅Na, 511.3399) in the positive HRFABMS, suggesting seven degrees of unsaturation. The IR spectrum indicated the presence of OH (3361 cm⁻¹) and C=O (1715, 1700 cm⁻¹) functionalities. The ¹³C NMR data (Table 1) of compound 3 resembled those of 2 except for resonances at δ_C 46.0 (C-22), 123.2 (C-23), 143.3 (C-24), 70.2 (C-25), 31.3 (C-26), and 31.2 (C-27). In the ¹H NMR spectrum (Table 1), a pair of olefinic

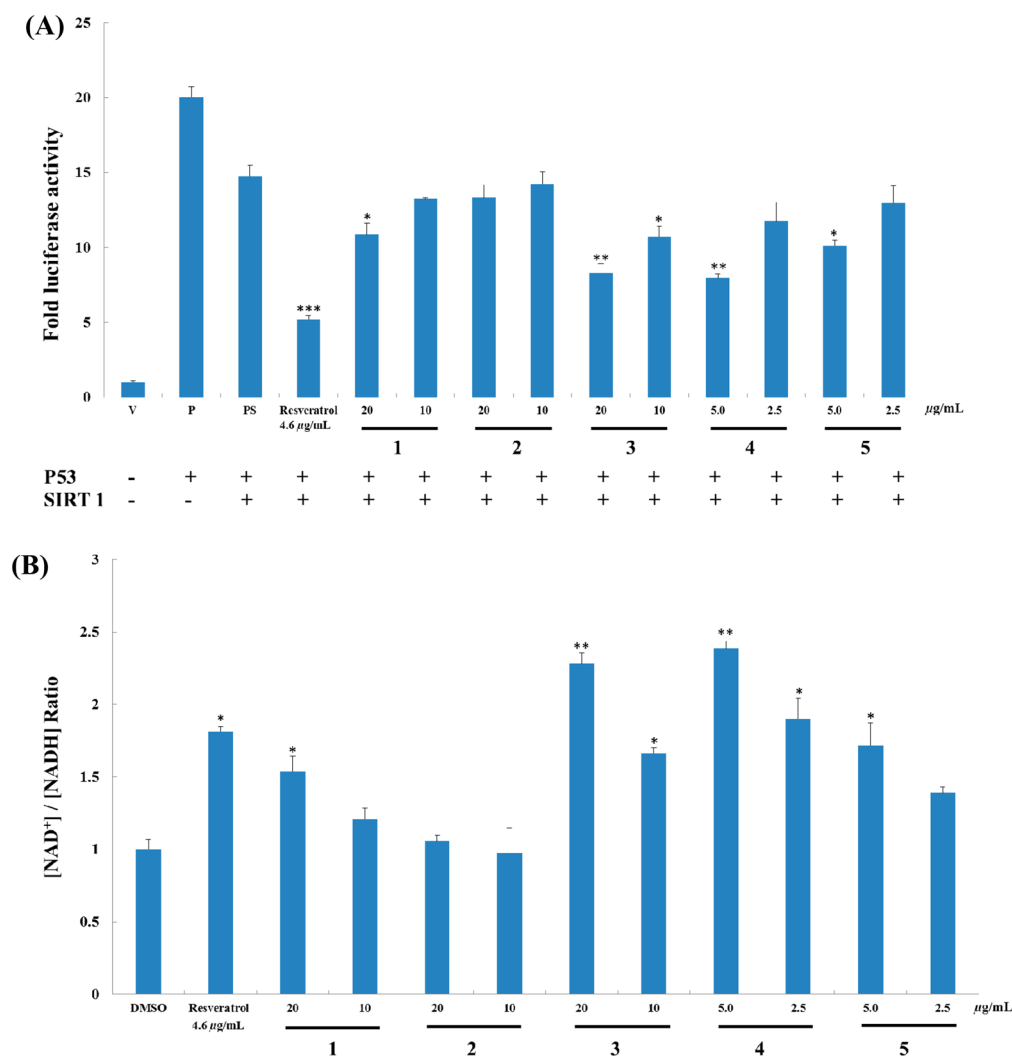


Figure 4. Effects of compounds 1–5 on SIRT1 activity in cell-based assays. (A) HEK293 cells were transiently transfected with p53-luc, myc-p53, and flag-SIRT1 plasmid as described in the Experimental Section. Following transfection, the cells were incubated with the compounds and resveratrol for 12 h. Compounds 1 and 3–5 were found to decrease the transcriptional activity of p53 in the HEK293 cells in a SIRT1-p53 luciferase cell-based assay. (B) Compounds 1 and 3–5 resulted in an increased intracellular NAD⁺/NADH ratio in HEK293 cells after 12 h treatment in a NAD⁺/NADH ratio cell-based assay.

protons at δ_{H} 6.25 (m) and 6.02 (d, $J = 15.4$ Hz) appeared instead of the $\Delta^{25,26}$ olefinic protons at δ_{H} 5.28 (br s) and 4.97 (br s) in **2**, and the oxymethine proton at $\delta_{\text{H}-24}$ 4.41 (br t, $J = 5.0$ Hz) of the latter compound also disappeared from the spectrum. These observations suggested the presence of a $\Delta^{23,24}$ olefinic system and an OH-25 group in **3**, which was confirmed by the following HMBC correlations (Figure 1): from H₃-26/27 (δ_{H} 1.53, 6H) to C-24 (δ_{C} 143.3) and C-25 (δ_{C} 70.2); and from H₂-22 (δ_{H} 2.61 and 2.54) to C-23 (δ_{C} 123.2) and C-24 (δ_{C} 143.3). The large coupling constant $J = 15.4$ Hz between H-23 and H-24 indicated an *E*-type $\Delta^{23,24}$ olefinic bond. Furthermore, the coupling constants between H-5 and H-6 ($J = 11.0$ Hz) and between H-13 and H-17 ($J = 10.0$ Hz), combined with the NOESY correlations (from H-6 to H₃-18, H₃-19, and H₃-29; from H-13 to H₃-18; and from H-17 to H₃-21 and H₃-30 (Figure 2)), aided in the determination of the α -oriented OH-6, the α -oriented H-17, and the C-20(*S*) configuration. Consequently, compound **3** was established as 6 α ,20(*S*),25-trihydroxydammar-3,12-dione-23-ene.

Compounds **1–3** were all found to possess a rare 3,12-dione-6-hydroxydammarane framework and together represent only

the second example of such a framework.²² The absolute configurations of compounds **2** and **3** were determined using a modified Mosher method in the present work.²⁹ Two portions of compound **2** (0.5 mg each) were treated with (*S*)-(+)- and (*R*)-(–)- α -methoxy- α -(trifluoromethyl)phenylacetyl chloride (MTPA-Cl, 5 μ L) in deuterated pyridine in separate NMR tubes, yielding the (*S*)- and (*R*)-MTPA ester derivatives at OH-6, respectively, whereas no esterification occurred at OH-24, based on the NMR and MS data analysis. The chemical shift differences $\Delta\delta = \delta_{\text{S}} - \delta_{\text{R}}$ were determined based on a ¹H–¹H COSY experiment. For H-5 and H₂-7, positive and negative $\Delta\delta$ values (Experimental Section) were observed, respectively. Therefore, the absolute configuration at C-6 was identified to be *S*.²⁹ Following the same procedure, the absolute configuration at C-6 in compound **3** was also determined as *S*. Because of the limited amount isolated in this investigation, the absolute configuration of compound **1** was not established. From a biogenetic viewpoint, compounds **1–3** most likely possess the same absolute configuration at C-6, due to their coexistence in the same plant.

The remaining two compounds, dammar-20(22),24-diene-3 β ,6 α ,12 β -triol (**4**)²⁰ and 20(S)-ginsenoside Rg₃ (**5**)²¹ were also isolated and identified based on the comparison of their spectroscopic data and optical rotations with literature values.

SIRT1 is a regulator in many metabolic responses via its deacetylase activity.³⁰ It selectively deacetylates the K382 residue of p53, consequently decreasing p53 transcriptional activity, to prevent DNA damage.³¹ The stimulatory effects of compounds **1**–**5** on SIRT1 activity were first examined using an in vitro SIRT1-NAD/NADH enzyme-based assay. As shown in Figure 3, compounds **1** and **3**–**5** increased significantly the SIRT1 deacetylase activities in a dose-dependent manner at 10 and 20 μ g/mL. Among them, compound **4** showed the most potent stimulatory effect. Next, the effects of the compounds on SIRT1 were examined using a SIRT1-p53 luciferase (Figure 4A) and NAD⁺/NADH ratio (Figure 4B) cell-based assays. As shown in Figure 4A, decreased p53 transcriptional activity was observed after treatment with compounds **1** and **3**–**5** in HEK293 cells that were transfected with p53-luc and SIRT1. In this assay, compounds **4** and **5** were tested at concentrations of 2.5 and 5 μ g/mL due to their cytotoxicity at higher concentrations. Because NAD⁺ functions as a substrate for SIRT1-mediated deacetylation, the stimulatory effects of compounds **1**–**5** on SIRT1 activity were confirmed via determining the NAD⁺ level using a NAD⁺/NADH ratio assay (Figure 4B). Results showed that compounds **1** and **3**–**5** increased significantly the intracellular NAD⁺/NADH ratio in HEK293 cells. Considering the critical role of NAD⁺ in SIRT1 deacetylase activity and the observed data, it is probable that the increase in SIRT1 activity by compounds **1** and **3**–**5** was accomplished by regulating the NAD⁺/NADH ratio.³²

How to control aging and longevity has long been a topic of considerable interest. Caloric restriction (CR) has shown the potential to extend lifespan and treat age-related diseases, with the NAD⁺/NADH ratio and SIR2 playing essential roles in this process.^{33,34} Although the causes of aging are still under debate, mitochondrial dysfunction has gained attention as the key hallmark. Aging leads to a specific loss of mitochondrial-encoded oxidative phosphorylation (OXPHOS) subunits. The depletion of the nuclear NAD⁺ level induces both reduction of the activity of SIRT1 and HIF1 α stabilization by decline of the Von Hippel-Lindau (VHL) E3 ubiquitin ligase, and these changes ultimately induce mitochondrial metabolism to enter into a chronically pseudohypoxic state during aging.³⁵ CR is known to delay many diseases associated with aging, including type 2 diabetes and cancer. Increasing NAD⁺ levels by CR recovers mitochondrial homeostasis, and experiments on 22-month-old mice treatment for 1 week with nicotinamide mononucleotide (NMN), a key NAD⁺ intermediate, reversed the reduction of VHL E3 ubiquitin ligase and accumulation of HIF-1 α .³⁵

In the present study, three new (**1**–**3**) and two known (**4** and **5**) dammarane triterpenes were isolated from *P. ginseng* leaves by bioassay-guided fractionation. Compounds **1** and **3**–**5** showed significant stimulatory effects on SIRT1 activity in luciferase assay and also increased the intracellular NAD⁺/NADH ratio in HEK293 cells. From a structural aspect, compounds **1**–**3** possess identical ring systems, differing only in their side chain functionalities. Thus, for the 3,12-dione-6-hydroxydammarane framework, it appears that the side-chain architecture has the main influence on the stimulatory effects to SIRT1 activity. 20(S)-Ginsenoside Rg₃ (**5**) and its optical isomer, 20(R)-ginsenoside Rg₃, have been reported to exhibit

different biological activities due to the opposite spatial arrangement of the hydroxy group at C-20.³⁶ Purified 20(R)-ginsenoside Rg₃ was obtained herein following a previously reported method,³⁷ and the stimulatory effects of 20(S)- and 20(R)-ginsenoside Rg₃ on SIRT1 activity were compared using a SIRT1-p53 luciferase cell-based assay. Results indicated that 20(R)-ginsenoside Rg₃ has a somewhat more potent stimulatory effect on SIRT1 deacetylase activity than 20(S)-ginsenoside Rg₃, in a dose-dependent manner (Supporting Information). It has been reported that *P. ginseng* treatment significantly increased the lifespan of the nematode *Caenorhabditis elegans*.³⁸ The present study indicated that this phenomenon may be due to the stimulatory effects of ginseng triterpenoids on SIRT1 activity.

■ EXPERIMENTAL SECTION

General Experimental Procedures. Optical rotations were determined on a JASCO P-2000 polarimeter (JASCO International Co. Ltd., Tokyo, Japan) using a 100 mm glass microcell. The IR spectra were measured by a Nicolet 6700 FT-IR (Thermo Electron Corp., Waltham, Massachusetts, U. S. A.). NMR spectra for compounds **1**–**5** were obtained in deuterated solvents containing TMS using a Varian Unity Inova 500 MHz spectrometer, for which experiments were conducted at the Korea Basic Science Institute, Gwangju Center, Korea. NMR spectra for MTPA esters of compounds **2** and **3** were recorded in C₅D₅N on a Bruker Avance 400 MHz spectrometer at the College of Pharmacy, Seoul National University, Seoul, Korea. HRFABMS and HRESIMS were determined using a JEOL JMS 700 (JEOL, Ltd., Tokyo, Japan) and an Agilent 6530 Q-TOF (Agilent Technologies, Inc., Santa Clara, California, U. S. A.) spectrometer, respectively, at the College of Pharmacy, Seoul National University, Seoul, Korea. Column chromatography (CC) was performed with silica gel (63–200 μ m particle size) and RP-C₁₈ (40–63 μ m particle size) obtained from Merck (Darmstadt, Germany), as well as Sephadex LH-20 (Sigma-Aldrich Corp., St. Louis, Missouri, U. S. A.). TLC was checked on RP-18 F₂₅₄ and silica gel 60 F₂₅₄ plates from Merck (Darmstadt, Germany). HPLC was performed on a Gilson system with a UV detector and Optima Pak C₁₈ column (10 \times 250 mm, 10 μ m particle size; RS Tech, Seoul, Korea). Analytical grade solvents were used for extraction and isolation.

Plant Material. *Panax ginseng* leaves were purchased from Mergens Co. (Suwon City, Gyeonggi-do, Republic of Korea) in November, 2010, and were authenticated by Professor Y. G. Kim at Seoul National University. A voucher specimen (SNU2010-10) was deposited at the College of Pharmacy, Seoul National University, Seoul, Korea.

Extraction and Isolation. The dried leaves of *P. ginseng* (206 g) were extracted with ethanol at room temperature for one week to give a crude ethanol extract of about 18.6 g after drying. This ethanol extract was subjected to liquid–liquid partitioning using hexane, EtOAc, *n*-BuOH, and H₂O. Screening indicated stimulatory effects on SIRT1 activity in the *n*-BuOH portion. Bioactivity-guided fractionation of the bioactive *n*-BuOH part (8.2 g) was performed using an in vitro SIRT1-NAD/NADH enzyme-based assay. Part of the *n*-BuOH fraction (6 g) was chromatographed over silica gel CC (2 \times 50 cm) and eluted with mixtures of CHCl₃/MeOH (20:0 \rightarrow 0:1) to yield eight fractions, F1–F8. Fraction F1 (503 mg) was chromatographed again over RP-C₁₈ CC (1 \times 30 cm), eluting with MeOH/H₂O (1:9 \rightarrow 9:1) to afford four subfractions (F1.1–

F1.4). Subfraction F1.3 (103 mg) was further chromatographed over LH-20 CC (1 × 30 cm) with MeOH to yield five subfractions (F1.3.1–F1.3.5). Subfraction F1.3.3 (23 mg) was purified by HPLC [mobile phase, MeOH in H₂O containing 0.1% HCO₂H (0–40 min, 62% MeOH); flow rate, 2 mL/min; UV detection at 205 and 254 nm] to give compounds **2** (*t_R* = 32 min, 1.9 mg) and **3** (*t_R* = 36 min, 2.3 mg). Subfraction F1.3.4 (20 mg) was purified by Sephadex LH-20 CC (1 × 20 cm) using MeOH/H₂O (1:1 → 1:0) to give compound **1** (1.0 mg). Subfraction F1.3.5 (19 mg) was also chromatographed over Sephadex LH-20 CC (1 × 20 cm) and eluted with MeOH to give compound **4** (3.1 mg). Fraction F3 (701 mg) was further chromatographed by silica gel CC (1 × 30 cm) and eluted with CH₂Cl₂/MeOH (40:1 → 0:1) to give six subfractions (F3.1–F3.6). Subfraction F3.2 (136 mg) was separated into seven subfractions (F3.2.1–F3.2.7) by Sephadex LH-20 CC (1 × 20 cm) eluted with MeOH. Compound **5** (*t_R* = 40 min, 3.3 mg) was purified from subfraction F3.2.4 (26 mg) by HPLC [mobile phase, MeOH in H₂O containing 0.1% HCO₂H (0–40 min, 80% MeOH); flow rate, 2 mL/min; UV detection at 205 and 254 nm].

6 α ,20(S)-Dihydroxydammar-3,12-dione-24-ene (1): white, amorphous powder; [α]_D²⁵ +25.0 (*c* 0.3, MeOH); IR (KBr) ν_{\max} 3397, 1722, 1705, 1654, 1381, 1182, 982, 905 cm⁻¹; ¹H and ¹³C NMR data, Table 1; HRFABMS *m/z* 495.3457 [M + Na]⁺ (calcd for C₃₀H₄₈O₄Na, 495.3450).

6 α ,20(S),24(S)-Trihydroxydammar-3,12-dione-25-ene (2): white, amorphous powder; [α]_D²⁵ –51.5 (*c* 0.2, MeOH); IR (KBr) ν_{\max} 3362, 2971, 1721, 1700, 1637, 1586, 1421, 1181, 1023, 905, 670 cm⁻¹; ¹H and ¹³C NMR data, Table 1; HRFABMS *m/z* 511.3409 [M + Na]⁺ (calcd for C₃₀H₄₈O₅Na, 511.3399).

6 α ,20(S),25-Trihydroxydammar-3,12-dione-23-ene (3): white, amorphous powder; [α]_D²⁵ +42.0 (*c* 0.3, MeOH); IR (KBr) ν_{\max} 3361, 2972, 1715, 1700, 1541, 1459, 1340, 1227, 1030, 926, 653 cm⁻¹; ¹H and ¹³C NMR data, Table 1; HRFABMS *m/z* 511.3346 [M + Na]⁺ (calcd for C₃₀H₄₈O₅Na, 511.3399).

Determination of the Absolute Configurations of 2 and 3 by the Modified Mosher Method. A sample of compound **2** (0.5 mg) was dissolved in deuterated pyridine and transferred into a dried NMR tube, after which (S)-(+)- α -methoxy- α -(trifluoromethyl)phenylacetyl chloride (5 μ L) was added under a N₂ gas stream. The NMR tube was kept at room temperature overnight. The same procedure was performed to obtain the (R)-MTPA ester of **2** by reaction of the compound with (R)-(–)- α -methoxy- α -(trifluoromethyl)phenylacetyl chloride (5 μ L). Based on ¹H–¹H COSY and MS experiments, the OH-6 group in **2** was esterified and chemical shifts of H-5, H-6, and H-7 for the (S)- and (R)-MTPA esters of **2** were determined. The (S)-MTPA ester of **2** produced the following data: δ_{H} (C₅D₅N, 400 MHz) 2.21 (H-5), 5.61 (H-6), 2.08 (H-7a), 1.61 (H-7b); HRESIMS *m/z* 727.3782 [M + Na]⁺ (calcd for C₄₀H₅₅F₃O₇Na, 727.3798). The (R)-MTPA ester of **2** resulted in the following: δ_{H} (C₅D₅N, 400 MHz) 2.19 (H-5), 5.51 (H-6), 2.15 (H-7a), 1.81 (H-7b); HRESIMS *m/z* 705.3950 [M + H]⁺ (calcd for C₄₀H₅₆F₃O₇, 705.3978), 727.3785 [M + Na]⁺ (calcd for C₄₀H₅₅F₃O₇Na, 727.3798).

The same preparation methods were used to produce the (S)- and (R)-MTPA esters of **3**. The (S)-MTPA ester of **3** yielded the following data: δ_{H} (C₅D₅N, 400 MHz) 2.21 (H-5), 5.62 (H-6), 2.13 (H-7a), 1.62 (H-7b); HRFABMS *m/z* 705.4005 [M + H]⁺ (calcd for C₄₀H₅₆F₃O₇, 705.3978). The

(R)-MTPA ester of **3** results were as follows: δ_{H} (C₅D₅N, 400 MHz) 2.20 (H-5), 5.55 (H-6), 2.15 (H-7a), 1.82 (H-7b); HRFABMS *m/z* 705.3962 [M + H]⁺ (calcd for C₄₀H₅₆F₃O₇, 705.3978).

Cell Culture and Transfection. HEK293 cells were kept in a 37 °C incubator with 5% CO₂ and cultured in DMEM containing 10% fetal bovine serum. The cells were placed in 24-well plates with a concentration of 10⁵ cells/1 mL medium in each well. After 24 h, the cells were transfected with 0.2 μ g PG13-luc plasmid, 0.2 μ g RSV- β -gal plasmid, 0.1 μ g myc-tagged p53 plasmid (myc-p53), and 0.2 μ g flag-tagged SIRT1 plasmid (flag-SIRT1) using the PEI transfection reagent (Polyscience, Inc., Warrington, PA, U. S. A.). The cultures were then maintained in DMEM medium without serum, and were treated with the compounds of interest after 24 h post-transfection.

In Vitro SIRT1 Deacetylation with a SIRT1-NAD/NADH Enzyme-Based Assay. The SIRT1 enzyme reaction was conducted with 25 μ L per well in a half-volume 96 well microplate. The SIRT1 reaction solution included 0.02 U/ μ L enzyme, with or without test compound, in SIRT1 assay buffer (1 mg/mL BSA, 1 mM MgCl₂, 2.7 mM KCl, 137 mM NaCl, and 50 mM Tris–HCl pH 8.0). The enzyme-compound mixture and the assay buffer (12.5 μ L) were incubated at room temperature for 5 min. The reaction was started with the addition of 12.5 μ L of a solution containing 500 μ M NAD⁺ and 100 μ M Fluor de Lys-SIRT1. After 1 h of incubation at room temperature, the reaction was quenched by adding 25 μ L of 1X Fluor de Lys Developer II with 2 mM nicotinamide in the HDAC assay buffer (1 mM MgCl₂, 2.7 mM KCl, 137 mM NaCl, and 50 mM Tris–HCl pH 8.0). After 30 min of incubation, the fluorescence of the reaction solution was measured using a SpectraMax GEMINI XPS microplate reader (Molecular Devices, Sunnyvale, CA, U. S. A.) with the excitation wavelength (360 nm) and emission (450 nm), after adding 50 μ L of the SIRT1 assay buffer. The positive and negative controls were the reaction with DMSO or without enzyme, respectively.

SIRT1 Deacetylation with a Luciferase Reporter Cell-Based Assay. Cells were transfected with PG13-luc (wt p53 binding sites) and the reporter plasmid, as well as with the plasmid encoding flag–flag-SIRT1 and the plasmid encoding myc-p53, with an internal control of the RSV- β -gal plasmid. The amount of transfected DNA in each well was the same. Using an analytical luminometer (Promega, Madison, WI, U. S. A.), the luciferase activity was measured based on the addition of 30 μ L of luciferin into 70 μ L of lysate. A Dual-Luciferase assay kit (Promega, Madison, WI, U. S. A.) was used for checking the promoter activity on the basis of measured renilla luciferase and luciferase. Cells were lysed and assayed for flag-SIRT1 reporter activities, namely, myc-p53 and p53, for which were corrected by constitutive β -galactosidase luciferase expression. Calculation of normalized values was performed by dividing the luciferase activity by the renilla luciferase activity.

NAD⁺/NADH Ratio Assay. The NAD⁺/NADH ratio was measured from whole-cell extracts of HEK293 cells using the Biovision NAD/NADH quantitation kit (Red Fluorescence, AAT Bioquest, Inc., Sunnyvale, CA, U. S. A.), according to the manufacturer's instructions.

Statistical Analysis. Statistical calculations were conducted in Microsoft Excel 2007. Results were given as the means \pm SD

of three to five independent experiments (* $p < 0.05$, ** $p < 0.01$, *** $p < 0.001$, compared to the control).

■ ASSOCIATED CONTENT

■ Supporting Information

1D (^1H and ^{13}C) and 2D (HSQC and HMBC) NMR spectra for compounds 1–3, HRESIMS data for (S)- and (R)-MTPA esters of compound 2, a figure showing dose-dependent effects of resveratrol on SIRT1 activity, and a figure showing the stimulation of SIRT1 deacetylase activity of 20(R)- and 20(S)-ginsenoside Rg₃ in a SIRT1-p53 luciferase cell-based assay. These materials are available free of charge via the Internet at <http://pubs.acs.org>.

■ AUTHOR INFORMATION

Corresponding Author

*W.-K. Oh. E-mail: wkohl@snu.ac.kr. Tel. and Fax: +82-02-880-7872.

Notes

The authors declare no competing financial interest.

■ ACKNOWLEDGMENTS

This work was supported in part by grants from the National Research Foundation of Korea (NRF) [(NRF-2012R1A2A2A01009417) and from the Procurement and Development of Foreign Biological Resources (2012-K1A1A3307871) funded by the Korean government.

■ REFERENCES

- (1) Napper, A. D.; Hixon, J.; McDonagh, T.; Keavey, K.; Pons, J. F.; Barker, J.; Yau, W. T.; Amouzegh, P.; Flegg, A.; Hamelin, E.; Thomas, R. J.; Kates, M.; Jones, S.; Navia, M. A.; Saunders, J. O.; DiStefano, P. S.; Curtis, R. *J. Med. Chem.* **2005**, *48*, 8045–8054.
- (2) Amagata, T.; Xiao, J.; Chen, Y. P.; Holsopple, N.; Oliver, A. G.; Gokey, T.; Guliaev, A. B.; Minoura, K. *J. Nat. Prod.* **2012**, *75*, 2193–2199.
- (3) Seo, J. S.; Moon, M. H.; Jeong, J. K.; Seol, J. W.; Lee, Y. J.; Park, B. H.; Park, S. Y. *Neurobiol. Aging* **2012**, *33*, 1110–1120.
- (4) Kim, E. J.; Kho, J. H.; Kang, M. R.; Um, S. *J. Mol. Cell* **2007**, *28*, 277–290.
- (5) Olmos, Y.; Brosens, J. J.; Lam, E. W. F. *Drug Resist. Updates* **2011**, *14*, 35–44.
- (6) Cohen, H. Y.; Miller, C.; Bitterman, K. J.; Wall, N. R.; Hekking, B.; Kessler, B.; Howitz, K. T.; Gorospe, M.; de Cabo, R.; Sinclair, D. A. *Science* **2004**, *305*, 390–392.
- (7) Blum, C. A.; Ellis, J. L.; Loh, C.; Ng, P. Y.; Perni, R. B.; Stein, R. L. *J. Med. Chem.* **2010**, *54*, 417–432.
- (8) Mai, A.; Valente, S.; Meade, S.; Carafa, V.; Tardugno, M.; Nebbioso, A.; Galmozzi, A.; Mitro, N.; De Fabiani, E.; Altucci, L.; Kazantsev, A. *J. Med. Chem.* **2009**, *52*, 5496–5504.
- (9) Bemis, J. E.; Vu, C. B.; Xie, R.; Nunes, J. J.; Ng, P. Y.; Disch, J. S.; Milne, J. C.; Carney, D. P.; Lynch, A. V.; Jin, L.; Smith, J. J.; Lavu, S.; Iffland, A.; Jirousek, M. R.; Perni, R. B. *Bioorg. Med. Chem. Lett.* **2009**, *19*, 2350–2353.
- (10) Vu, C. B.; Bemis, J. E.; Disch, J. S.; Ng, P. Y.; Nunes, J. J.; Milne, J. C.; Carney, D. P.; Lynch, A. V.; Smith, J. J.; Lavu, S.; Lambert, P. D.; Gagne, D. J.; Jirousek, M. R.; Schenk, S.; Olefsky, J. M.; Perni, R. B. *J. Med. Chem.* **2009**, *52*, 1275–1283.
- (11) Davis, J. M.; Murphy, E. A.; Carmichael, M. D.; Davis, B. *Am. J. Physiol.: Regul., Integr. Comp. Physiol.* **2009**, *296*, R1071–R1077.
- (12) Pervaiz, S.; Holme, A. L. *Antioxid. Redox Signaling* **2009**, *11*, 2851–2897.
- (13) Baur, J. A.; Pearson, K. J.; Price, N. L.; Jamieson, H. A.; Lerin, C.; Kalra, A.; Prabhu, V. V.; Allard, J. S.; Lopez-Lluch, G.; Lewis, K.; Pistell, P. J.; Poosala, S.; Becker, K. G.; Boss, O.; Gwinn, D.; Wang, M.; Ramaswamy, S.; Fishbein, K. W.; Spencer, R. G.; Lakatta, E. G.; Le

Couteur, D.; Shaw, R. J.; Navas, P.; Puigserver, P.; Ingram, D. K.; de Cabo, R.; Sinclair, D. A. *Nature* **2006**, *444*, 337–342.

(14) Hubbard, B. P.; Gomes, A. P.; Dai, H.; Li, J.; Case, A. W.; Considine, T.; Riera, T. V.; Lee, J. E.; Lamming, D. W.; Pentelute, B. L.; Schuman, E. R.; Stevens, L. A.; Ling, A. J.; Armour, S. M.; Michan, S.; Zhao, H.; Jiang, Y.; Sweitzer, S. M.; Blum, C. A.; Disch, J. S.; Ng, P. Y.; Howitz, K. T.; Rolo, A. P.; Hamuro, Y.; Moss, J.; Perni, R. B.; Ellis, J. L.; Vlasuk, G. P.; Sinclair, D. A. *Science* **2013**, *339*, 1216–1219.

(15) Dao, T. T.; Tran, T. L.; Kim, J.; Nguyen, P. H.; Lee, E. H.; Park, J.; Jang, I. S.; Oh, W. K. *J. Nat. Prod.* **2012**, *75*, 1332–1338.

(16) Hwang, H. J.; Kim, E. H.; Cho, Y. D. *Phytochemistry* **2001**, *58*, 1015–1024.

(17) Mallol, A.; Cusidó, R. M.; Palazón, J.; Bonfill, M.; Morales, C.; Piñol, M. T. *Phytochemistry* **2001**, *57*, 365–371.

(18) Schlag, E. M.; McIntosh, M. S. *Phytochemistry* **2006**, *67*, 1510–1519.

(19) Hong, S. Y.; Kim, J. Y.; Ahn, H. Y.; Shin, J.; Kwon, O. J. *Agric. Food Chem.* **2012**, *60*, 3086–3091.

(20) Wu, L. J.; Wang, L. B.; Gao, H. Y.; Wu, B.; Song, X. M.; Tang, Z. S. *Fitoterapia* **2007**, *78*, 556–560.

(21) Cheng, L. Q.; Na, J. R.; Bang, M. H.; Kim, M. K.; Yang, D. C. *Phytochemistry* **2008**, *69*, 218–224.

(22) Sugimoto, S.; Nakamura, S.; Matsuda, H.; Kitagawa, N.; Yoshikawa, M. *Chem. Pharm. Bull.* **2009**, *57*, 283–287.

(23) Yahara, S.; Tanaka, O.; Nishioka, I. *Chem. Pharm. Bull.* **1978**, *26*, 3010–3016.

(24) Bedir, E.; Toyang, N. J.; Khan, I. A.; Walker, L. A.; Clark, A. M. *J. Nat. Prod.* **2001**, *64*, 95–97.

(25) Yin, F.; Zhang, Y.; Yang, Z.; Cheng, Q.; Hu, L. *J. Nat. Prod.* **2006**, *69*, 1394–1398.

(26) Yin, F.; Hu, L.; Lou, F.; Pan, R. *J. Nat. Prod.* **2004**, *67*, 942–952.

(27) Malinovsky, G. V.; Novikov, V. L.; Denisenko, V. A.; Uvarova, N. I. *Chem. Nat. Compd.* **1980**, *16*, 257–261.

(28) Lee, I. S.; Oh, S.-R.; Ahn, K.-S.; Lee, H.-K. *Chem. Pharm. Bull.* **2001**, *49*, 1024–1026.

(29) (a) Su, B. N.; Park, E. J.; Mbawambo, Z. H.; Santarsiero, B. D.; Mesecar, A. D.; Fong, H. H. S.; Pezzuto, J. M.; Kinghorn, A. D. *J. Nat. Prod.* **2002**, *56*, 1278–1282. (b) Chin, Y.-W.; Salim, A. A.; Su, B. N.; Mi, Q.; Chai, H. B.; Riswan, S.; Kardono, L. B. S.; Ruskandi, A.; Farnsworth, N. R.; Swanson, S. M.; Kinghorn, A. D. *J. Nat. Prod.* **2008**, *71*, 390–395. (c) Pan, L.; Yong, Y.; Deng, Y.; Lantvit, D. D.; Ninh, T. N.; Chai, H.; de Blanco, E. J. C.; Soejarto, D. D.; Swanson, S. M.; Kinghorn, A. D. *J. Nat. Prod.* **2012**, *75*, 444–452. (d) Chang, Y. C.; Deng, T. S.; Pang, K. L.; Hsiao, C. J.; Chen, Y. Y.; Tang, S. J.; Lee, T. H. *J. Nat. Prod.* **2013**, *76*, 1796–1800.

(30) Leibiger, I. B.; Berggren, P.-O. *Nat. Med.* **2006**, *12*, 34–36.

(31) (a) Milne, J. C.; Lambert, P. D.; Schenk, S.; Carney, D. P.; Smith, J. J.; Gagne, D. J.; Jin, L.; Boss, O.; Perni, R. B.; Vu, C. B.; Bemis, J. E.; Xie, R.; Disch, J. S.; Ng, P. Y.; Nunes, J. J.; Lynch, A. V.; Yang, H.; Galonek, H.; Israelian, K.; Choy, W.; Iffland, A.; Lavu, S.; Medvedik, O.; Sinclair, D. A.; Olefsky, J. M.; Jirousek, M. R.; Elliott, P. J.; Westpha, C. H. *Nature* **2007**, *450*, 712–716. (b) Saunders, L. R.; Verdin, E. *Science* **2009**, *323*, 1021–1022. (c) Botta, G.; De Santis, L. P.; Saladino, R. *Curr. Med. Chem.* **2012**, *19*, 5871–5884.

(32) (a) Couzin, J. *Science* **2004**, *303*, 1276–1279. (b) Cantó, C.; Gerhart-Hines, Z.; Feige, J. N.; Lagouge, M.; Noriega, L.; Milne, J. C.; Elliott, P. J.; Puigserver, P.; Auwerx, J. *Nature* **2009**, *458*, 1056–1060. (c) de Cabo, R.; Siendones, E.; Minor, R.; Navas, P. *Aging* **2010**, *2*, 63–68. (d) Chalkiadaki, A.; Guarente, L. *Nat. Rev. Endocrinol.* **2012**, *8*, 287–296.

(33) Lin, S. J.; Guarente, L. *Curr. Opin. Cell Biol.* **2003**, *15*, 241–246.

(34) (a) Pallàs, M.; Verdager, E.; Tajas, M.; Gutierrez-Cuesta, J.; Camins, A. *Recent Pat. CNS Drug Discovery* **2008**, *3*, 61–69. (b) Satoh, A.; Brace, C. S.; Rensing, N.; Clifton, P.; Wozniak, D. F.; Herzog, E. D.; Yamada, K. A.; Imai, S.-I. *Cell Metabol.* **2013**, *18*, 416–430.

(35) Gomes, A. P.; Price, N. L.; Ling, A. J.; Moslehi, J. J.; Montgomey, M. K.; Rajman, L.; White, J. P.; Teodoro, J. S.; Wrann, C. D.; Hubbard, B. P.; Mercken, B. P.; Palmeira, C. M.; de Cabo, R.

Rolo, A. P.; Turner, N.; Bell, E. L.; Sinclair, D. A. *Cell* **2013**, *155*, 1624–1638.

(36) Cheng, L.-Q.; Na, J. R.; Bang, M. H.; Kim, M. K.; Yang, D.-C. *Phytochemistry* **2008**, *69*, 218–224.

(37) Sun, C.; Gao, W.; Zhao, B.; Cheng, L. *Fitoterapia* **2013**, *84*, 213–221.

(38) Yu, Y.-B.; Dosanjh, L.; Lao, L.; Tan, M.; Shim, B. S.; Luo, Y. *PLoS One* **2010**, *5*, e9339, 1–10..